

Efficiency of Concrete Removal With a Pulsed Nd:YAG Laser

Michael Savina¹, Zhiyue Xu², Yong Wang², Claude Reed², Michael Pellin¹

¹Materials Science and Chemistry Divisions, Argonne National Laboratory, Argonne, Illinois, 60439

²Technology Development Division, Argonne National Laboratory, Argonne, Illinois, 60439

Submitted for publication in *Journal of Laser Applications*, May 2000

Abstract

The mechanism and efficiency of ablating concrete surfaces with a pulsed Nd:YAG laser were studied. Ablation efficiency and material removal rates were determined as functions of irradiance and pulse overlap. The ablation mechanism was dominated by fragmentation and disaggregation of the concrete. The ablation efficiency was insensitive to peak laser irradiance over a range from 0.2 to 4.4 MW/cm². Excessive pulse overlap (>60%) caused a significant decrease in ablation efficiency by inducing melting. In concrete samples, the cement phase of the material responds in various ways to the laser energy, including disaggregation, melting, and vaporization, but the aggregate portion (sand and rock) mostly fragments. The ablation effluent therefore consists of both micron-size aerosol particles and chunks of fragmented aggregate material.

This manuscript has been created by the University of Chicago as Operator of Argonne National Laboratory ("Argonne") under Contract No. W-31-109-ENG-38 with the U.S. Department of Energy. The U.S. Government retains for itself, and others acting on its behalf, a paid-up, nonexclusive, irrevocable worldwide license in said article to reproduce, prepare derivative works, distribute copies to the public, and perform publicly and display publicly, by or on behalf of the Government.

Introduction

The U.S. Department of Energy's nuclear weapons complex, a nation-wide system of facilities for research and production of nuclear materials and weapons, contains large amounts of radioactively contaminated concrete. This material is part of the legacy of the Cold War, and must be disposed of prior to the decommissioning of the various sites. In many cases the radiation levels emitted by these materials will remain dangerous for thousands of years, so that after the facility has been decommissioned the material from it must be stored and monitored over a very long period. Often the radioactive contaminants in concrete occupy only the surface and near-surface (~3-6 mm deep) regions of the material. Since many of the structures such as walls and floors are 30 cm or more thick, it makes environmental and economic sense to try to remove and store only the thin contaminated layer rather than to treat the entire structure as nuclear waste. Current mechanical removal methods, known as scabbling, are slow and labor intensive, suffer from dust control problems, and expose workers to radiation fields. Improved removal methods are thus in demand.

Laser ablation has previously been investigated as a means of concrete surface removal¹⁻⁶. Lasers are attractive since the power can be delivered remotely via articulated mirrors or fiber optic cables and the ablation head can be manipulated by robots, thus avoiding exposing workers and the laser system to the radiation field. In addition, lasers can be instrumented with emission spectrometers or effluent sampling devices to provide on-line analysis. In contrast to mechanical scabbling systems, laser beams can penetrate cracks or follow very rough or irregularly shaped surfaces. Finally, a laser ablation system produces the smallest possible waste stream since no

cleaning agents such as detergents or grit (from grit blasting systems) are mixed with the effluent.

Multi-kilowatt Nd:YAG and CO₂ lasers are capable of ablating concrete surfaces and affecting decontamination. Both cw^{1,2} and pulsed^{3,4} systems have been investigated, with the main difference lying in the mechanism of ablation. Pulsed systems rely on the shock heating produced in a small volume of rapidly heated material to disaggregate and explosively remove concrete, while cw systems rely on the differential thermal expansion of the various components of concrete (i.e. cement, sand, and aggregate) to induce thermal stress in a larger volume, which results in the fracture and removal of material.

This paper describes the ablation of cement and concrete by a 1.6 kW pulsed Nd:YAG laser. Ablation efficiency and material removal rates were determined as functions of irradiance and pulse overlap. The ablated surfaces and effluent were analyzed to determine ablation mechanisms and optimize the process. The results show that while the majority of the concrete ablates by shock-induced fracture and disaggregation, some of the cement phase of the concrete melts and vaporizes and produces a fine aerosol. Thus the effluent consists of both micron-size cement aerosol particles and larger chunks of fragmented aggregate material.

Experimental

Laser ablation experiments were conducted with the 1064 nm fundamental of an Electroxx 1.6 kW pulsed Nd:YAG laser. The system produced pulses of 0.5 to 1 ms duration with a nearly

square temporal profile. The pulse energies ranged up to 30 J depending on the operating mode and repetition rate, which ranged as high as 800 Hz. The beam was delivered via a 1 mm diameter fiber optic cable 10 m in length. Focal plane spot diameters ranged from 0.55 to 0.96 mm. The sample stage was moved in three dimensions under the stationary beam. A modest N₂ gas flow was maintained over the focussing lens to keep it free of debris.

Samples consisted of a 60/40 (wt/wt) mixture of sand and Type I Portland cement cast at a water/cement ratio of 0.5 and allowed to cure for at least thirty days prior to use. In addition, samples of high density concrete from a nuclear reactor at Argonne National Laboratory (Experimental Boiling Water Reactor) were ablated for comparison with the laboratory-produced material. Aerosol particle size distribution analysis was done with a seven stage particle impactor described previously⁴. Ablated surfaces and effluent were examined with optical microscopy.

Results

Ablation efficiency, defined here as the mass of material removed per unit energy delivered, was determined under varying conditions. Figure 1 shows the effect of pulse overlap, defined as the linear overlap distance of two consecutive pulses. These experiments were done at 800 Hz with 0.5 ms pulses, with the beam focused to 0.55 mm at the sample surface. Ablation efficiency was constant at about 0.2 mg/J for overlaps from 0 to 60%, but dropped as the overlap increased beyond 60%. Figure 2 is a photograph showing (clockwise from left) regions of the sample ablated at 0, 60, 80, and 90% linear pulse overlap. As implied by the efficiency data of

Figure 1, the width and depth of the ablated groove increased as the overlap increased up to about 60%, at which point the increase in groove volume no longer compensated for the increase in overlap and led to a decline in ablation efficiency. Figures 3-5 are optical micrographs of the 0, 60, and 90% overlap cases. In Figure 3(0% linear overlap) the surface is grainy, and shows sand grains and holes left behind after the removal of individual sand grains. In Figure 4 (60% linear overlap) the grooves are clearly deeper, but have rounded edges and smoother bottoms indicative of melting. In Figure 5 (90% linear overlap) the surface is glazed over with melted material.

Under pulsed laser ablation, concrete will fracture along a surface across which the induced stress due to differential thermal expansion exceeds the tensile strength. For the thermal shock mechanism to remove material efficiently, the final temperature of the material must be below the melting point so that 1) energy is not wasted in the solid-liquid phase transition, and 2) the material cannot accommodate the induced stress by viscous flow. This is demonstrated by the fact that the onset of melting observed at 60 % linear overlap in Figure 4 correlates with the drop in ablation efficiency seen in Figure 1. Melting can be induced by slow heating, in which the temperature gradient (and hence thermally induced stress) is lowered by heat flow out of the irradiated volume, or by irradiating an already hot surface so that the melting point is reached before the stress build-up is sufficient to fracture the material.

In the present study, the heating rates induced by laser pulses on cold (room temperature) surfaces were always sufficiently high to avoid melting (see Figure 6 and discussion below). Therefore the melting observed in Figures 4 and 5 is due to depositing laser energy on a hot surface, the source of the heat being the previous laser pulse. At linear pulse overlaps of less

than 50%, no part of the surface receives more than two consecutive pulses, the average exposure is 1.8 pulses and no melting is observed in the substrate, i.e. on the bulk side of the fracture surface. At 60% overlap some areas receive three consecutive pulses, with an average exposure of 2.3 pulses, and some melting is evident. Thus, the amount of laser energy that is deposited on the substrate side of the fracture surface, either directly from the laser pulse or via heat flow out of the ablated volume before the material leaves the surface, is low enough that three consecutive pulses are required to heat the material to melting. At 90% overlap (Figure 5) every point in the ablation groove receives at least four consecutive pulses and most of the track receives seven or more. The average exposure is 8.8 pulses, and extensive melting is noted and ablation efficiency is drastically lowered.

Figure 6 shows the effect of the peak laser irradiance on the ablation rate. The sample was ablated with either 0.5 or 1 ms pulses at a spot size of 0.95 mm and pulse overlap of 0% with the beam focal plane at the surface of the sample. The irradiance was varied by changing the pulse peak power from 1.4 to 30.2 kW, and the repetition rate was either 50, 100, or 200 Hz depending on the peak power. As shown in Figure 6, the relationship between ablation rate - expressed as the mass of material removed per laser pulse - and the peak irradiance is linear. This means that the ablation efficiency - expressed as the mass of material removed per unit of optical energy delivered - is constant over the range of irradiances from 0.2 to 4.4 MW/cm². The constant efficiency implies strongly that the mechanism of ablation is unchanged over this range of irradiance values and that factors such as melting or plasma shielding are unimportant or at least unchanging over this range. Thus the ablation rate depends only on the rate of energy delivery to the surface, i.e. on the average laser power. The slope of a linear fit to the data of

Figure 6 yields (with appropriate unit conversion) an ablation efficiency of 0.23 mg/J. From this value the concrete removal rate for any pulsed Nd:YAG with a similar temporal pulse profile can be calculated directly from the average laser power. For example, with the beam focused on the sample surface, this 1.6 kW Nd:YAG system is capable of a maximum ablation rate of 370 mg/s.

The efficiency value of 0.23 mg/J is higher than that obtained in the overlap data of Figure 1. This is most likely due to differences in the samples and day to day differences in laser performance. The data of Figure 6 were obtained from three different samples on three different days, and therefore constitute a more representative sampling than do the data of Figure 1.

Samples of high density concrete from a nuclear reactor (non-contaminated) were ablated for comparison with the laboratory samples of 60/40 sand/cement. The main differences between the samples were that the high density concrete contained large aggregate particles (rocks) which were absent in the laboratory samples, and had much less cement (10 to 15%, compared to 40% for the laboratory samples). The ablation efficiency obtained from high density concrete was 0.16 to 0.18 mg/J depending on the surface smoothness of the sample. The lower overall values are probably due to the presence of large aggregate particles (i.e. rocks) which tended to melt more readily than sand or cement. These findings are preliminary, coming from ablation runs with relatively high overlap (~50%), and suggest that for high density concrete the overlap must be kept lower than for the laboratory samples.

Our previous studies showed that cement and aggregate behave differently under high power pulsed irradiation⁴. Sand particles, which are generally on the order the same size as the

focused beam, i.e. about 1 mm, tend to fracture or dislodge without melting. Figure 7 shows a portion of the effluent from the ablation of a 60/40 sand/cement sample. The larger, smoother particles are fractured sand grains. The bulk of the stored nuclear waste from an ablation process would take this form, that is small, relatively unprocessed particles. Cement, which is a grainy material composed of particles up to a few tens of microns in size, reacts to the optical energy in several ways. While most of it tends to disaggregate into grainy clumps such as those seen in Figure 7, some of it melts or vaporizes. Much of the melted material spatters off the surface and forms aerosol particles along with the condensate from the vaporized material.

Though the aerosol portion makes up a small fraction of the total effluent, is important for several reasons. It is derived from the cement portion of the concrete, which is the phase that contains the radioactive contaminants, and is therefore a concentrated form of the contaminated concrete. Second, it constitutes the worst health hazard generated from the process, because the fine particles remain airborne much longer than the larger grains and represent a greater inhalation hazard. Any vacuum shroud/filtration system must be designed to collect these particles very efficiently. Finally, the aerosol phase and the vapor from which it is derived are the most amenable portions of the effluent for sampling and on-line analysis.

Figure 8 shows the aerosol aerodynamic particle size distribution obtained from the impactor. The distribution is bimodal, with a minimum at about one micron. Previous studies⁴ have shown that the smaller particles are preferentially enriched in aluminum, which is a minor constituent of Portland cement⁷. Together with the bimodal size distribution, this suggests that the smaller particles are formed primarily from the vapor phase (nucleated by an aluminum-rich

chemical phase) and the larger particles, many of which are hollow, are formed primarily from the melt/spatter process. These findings are important because they imply a thermal processing of the material which leads to chemical segregation. Characterization of this portion of the effluent is therefore important in designing effective waste handling and storage strategies.

Conclusions

Pulsed heating of concrete on the millisecond time scale with a Nd:YAG laser results in ablation via a thermal shock mechanism provided that the linear pulse overlap remains below ~60%. Above 60% overlap, residual heat from previous laser pulses causes melting which competes with ablation and lowers the material removal efficiency. At low overlap, the thermal shock mechanism dominates the laser-material interaction over the irradiance range studied (0.2 to 4.4 MW/cm²), resulting in constant material removal efficiency 0.23 mg/J for test samples consisting of 60/40 sand/cement. High density concrete ablated with lower efficiency, due at least in part to a greater tendency toward melting. Efficient ablation produces an effluent containing primarily fractured and disaggregated particles, however a small portion of the effluent is aerosol particles with diameters down to sub-micron. The size distribution and aluminum content of the particles suggest that two mechanisms are responsible for aerosol formation, namely melt/spatter for larger particles and vaporization/condensation for smaller particles.

Acknowledgements

The authors thank Dr. Keng Leong of Pennsylvania State University for many helpful discussions. This work was supported by the U.S. Department of Energy, BES-Materials Science, under Contract W-31-109-ENG-38; and by the U.S. Department of Energy, Environmental Management Science Program, under Contract W-31-109-ENG-38.

References

- 1) E.P. Johnston, G. Shannon, W.M. Steen, D.R. Jones and J.T. Spencer, ICALEO '98, Laser Institute of America, Volume 85a, 210-218, 1998.
 - 2) L. Li, P.J. Modern and W.M. Steen, *Concrete decontamination by laser surface treatment*, European patent No.94307937.6.
 - 3) M.R. Savina, Z. Xu, Y. Wang, M.P. Pellin, and K. Leong, ICALEO '98, Laser Institute of America, Volume 85a, 219-226, 1998.
 - 4) M.R. Savina, Z. Xu, Y. Wang, M.P. Pellin, and K. Leong, *J. Laser Appl.* **11** (6) 284-287 (1999).
 - 5) D.J. Flesher in *Elevated Temperature Coatings: Science and Technology I*, N.B. Dahotre, J.M. Hampikian, and J.J. Stiglich, Eds.; The Minerals, Metals, and Materials Society, 1995, 379-383.
 - 6) N.S. Cannon and D.J. Flesher in *Elevated Temperature Coatings: Science and Technology I*, N.B. Dahotre, J.M. Hampikian, and J.J. Stiglich, Eds.; The Minerals, Metals, and Materials Society, 1995, 385-91.
 - 7) H.F.W. Taylor, *The Chemistry of Cements*, Vol. 1, Academic Press, 1964.
- M. Savina, et. al; submitted for publication in *Journal of Laser Applications*, May 2000

Figure Captions

Figure 1: Concrete ablation efficiency as a function of linear pulse overlap. The overlap was adjusted by varying the speed of the sample under the beam.

Figure 2: Photograph of an ablated sample of 60/40 sand/cement. The ablated regions had pulse overlaps of (clockwise from left) 0, 60, 80, and 90%. The field of view is $\sim 7 \times 5$ mm. The ablation grooves are ~ 0.5 mm wide.

Figure 3: Optical micrograph of the surface of a 60/40 sand/cement sample after ablation at 0% pulse overlap. The field of view is $\sim 3 \times 4$ mm. The large, smooth particles are sand grains. The surface shows pits where individual sand grains have spalled off the surface.

Figure 4: Optical micrograph of the surface of a 60/40 sand/cement sample after ablation at 60% pulse overlap. The field of view is $\sim 4 \times 5.5$ mm. The ablation grooves are much deeper than the 0% overlap case (Figure 3), and virtually all the sand grains in the grooves have been removed by the laser. Some slight melting is evident in the rounded groove edges.

Figure 5: Optical micrograph of the surface of a 60/40 sand/cement sample after ablation at 90% pulse overlap. The field of view is $\sim 3 \times 4$ mm. A great deal of melting is evident compared to the lower overlap cases of Figures 3 and 4.

Figure 6: Concrete removal rate as a function of irradiance at 0% linear pulse overlap. Irradiance was varied by changing either the pulse energy and/or duration.

M. Savina, et. al; submitted for publication in *Journal of Laser Applications*, May 2000

Figure 7: Optical micrograph of the major portion of the effluent from ablation of concrete.

Figure 8: Aerodynamic particle size distribution of the aerosol portion of the concrete ablation effluent, obtained by sampling the effluent with a seven stage particle impactor.

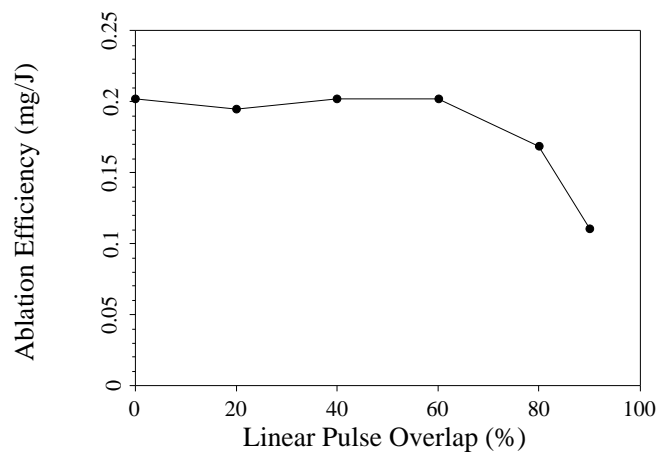


Figure 1

Michael Savina

Journal of Laser Applications

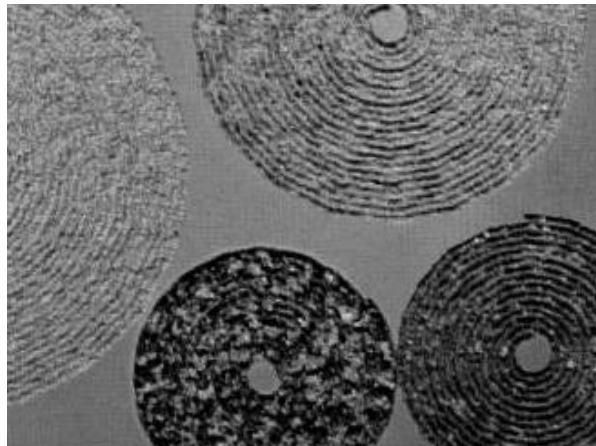


Figure 2

Michael Savina

Journal of Laser Applications

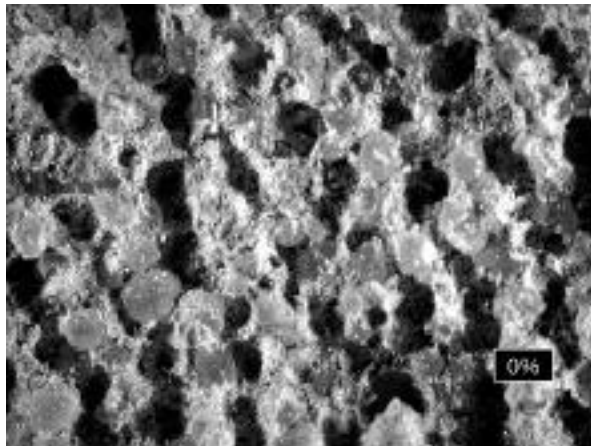


Figure 3

Michael Savina

Journal of Laser Applications

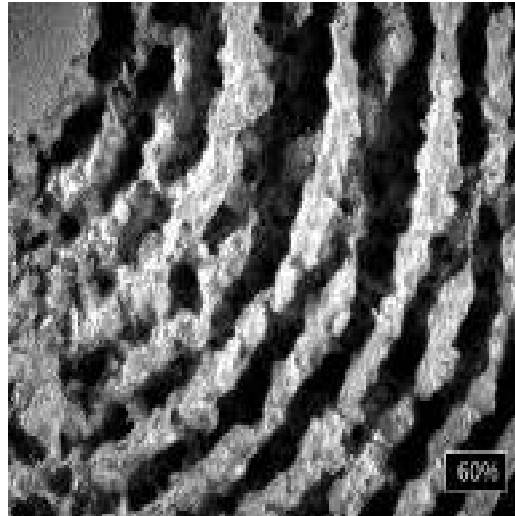


Figure 4

Michael Savina

Journal of Laser Applications

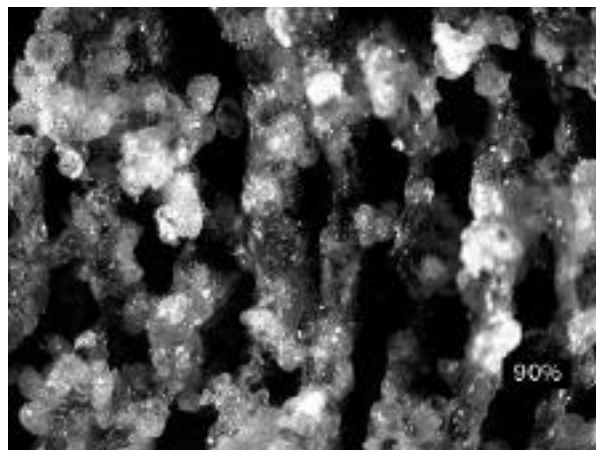


Figure 5

Michael Savina

Journal of Laser Applications

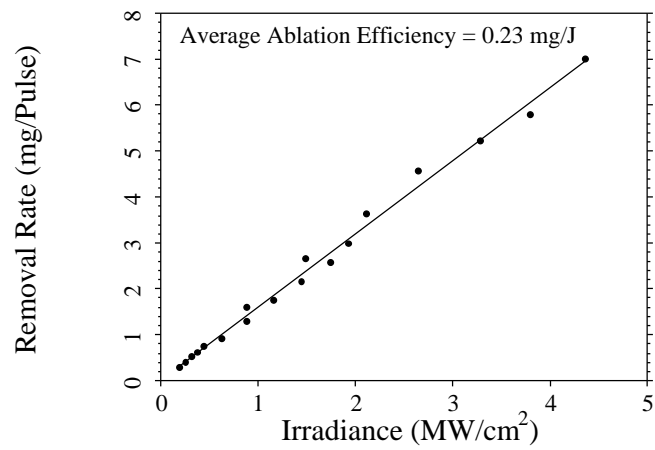


Figure 6

Michael Savina

Journal of Laser Applications

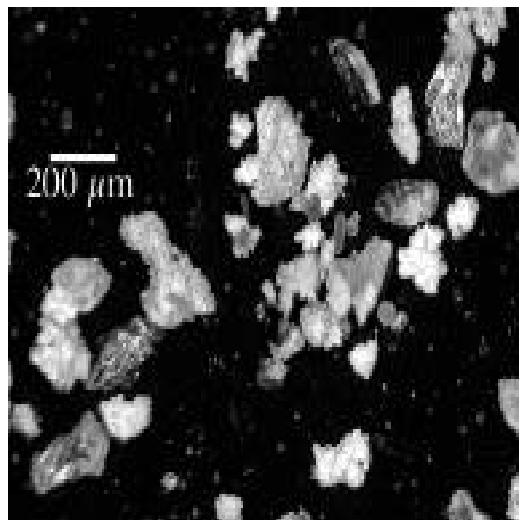


Figure 7

Michael Savina

Journal of Laser Applications

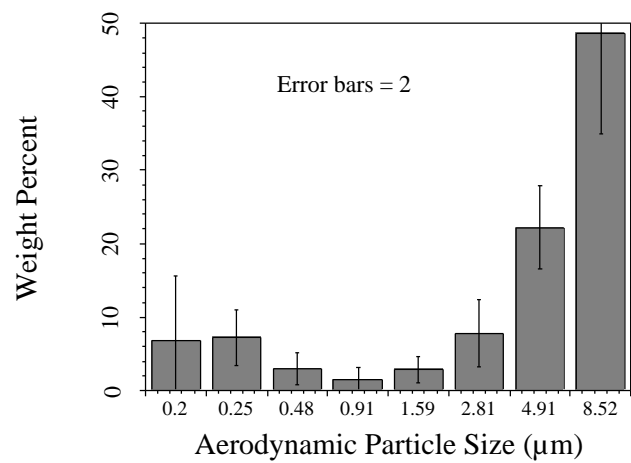


Figure 8

Michael Savina

Journal of Laser Applications